

SCIENTIFIC REPORTS



OPEN

Mutations underlying Episodic Ataxia type-1 antagonize Kv1.1 RNA editing

Elizabeth A. Ferrick-Kiddie¹, Joshua J. C. Rosenthal^{2,3}, Gregory D. Ayers⁴ & Ronald B. Emeson^{1,5}

Received: 11 October 2016
Accepted: 14 December 2016
Published: 20 February 2017

Adenosine-to-inosine RNA editing in transcripts encoding the voltage-gated potassium channel Kv1.1 converts an isoleucine to valine codon for amino acid 400, speeding channel recovery from inactivation. Numerous Kv1.1 mutations have been associated with the human disorder Episodic Ataxia Type-1 (EA1), characterized by stress-induced ataxia, myokymia, and increased prevalence of seizures. Three EA1 mutations, V404I, I407M, and V408A, are located within the RNA duplex structure required for RNA editing. Each mutation decreased RNA editing both *in vitro* and using an *in vivo* mouse model bearing the V408A allele. Editing of transcripts encoding mutant channels affects numerous biophysical properties including channel opening, closing, and inactivation. Thus EA1 symptoms could be influenced not only by the direct effects of the mutations on channel properties, but also by their influence on RNA editing. These studies provide the first evidence that mutations associated with human genetic disorders can affect *cis*-regulatory elements to alter RNA editing.

The Kv1.1 voltage-gated potassium (Kv) channel α -subunit plays an important role in regulating neuronal excitability. By dampening excitability at the axon initial segment and juxtaparanodal region¹, it can influence action potential initiation, propagation and reduce nerve terminal excitability, permitting fine-tuning of neurotransmitter release². Underscoring its physiological importance, genetic knockout studies have revealed that mice lacking Kv1.1 expression develop spontaneous seizures, hyperalgesia, and neurogenic cardiac dysfunction^{3–5}. Although Kv1.1 can form functional homotetrameric channels, Kv1.1 is predominantly found in heterotetramers with other Kv1 family members that contribute to a large diversity of Kv1 channel kinetics and pharmacology throughout the mammalian central nervous system^{6–9}. Further regulation of Kv1 channels is mediated through co-assembly with four accessory Kv β -subunits^{10,11}, where an inactivating domain in the Kv β amino terminus binds to the inner vestibule of the channel pore to block current flow, a process known as fast (N-type) inactivation^{12,13}.

RNA transcripts encoding Kv1.1 are modified by a site-specific adenosine-to-inosine (A-to-I) RNA editing event in which a genomically-encoded isoleucine (AUU) is converted to a valine (IUU) codon at amino acid position 400 of the protein¹⁴. This amino acid lies within the S6 transmembrane domain predicted to line the ion-conducting pore of the channel. Editing of Kv1.1 transcripts is dependent upon a region of double-stranded RNA (dsRNA) formed by intramolecular base-pairing interactions between imperfect, inverted repeat elements surrounding the targeted adenosine moiety¹⁵. This process is catalyzed by ADAR2, a member of a family of dsRNA-specific adenosine deaminases (ADARs)^{15,16}. Previous studies have revealed that Kv1.1 channels containing edited [Kv1.1(V)] subunits display a 20-fold faster rate of recovery from Kv β 1.1-inactivation, compared to non-edited channels [Kv1.1(I)]¹⁵. More recent studies have indicated that only small alterations in the hydrophobicity of the editing site amino acid were needed to reproduce the editing-dependent alterations in recovery kinetics¹⁷.

¹Department of Molecular Physiology & Biophysics, Vanderbilt University School of Medicine, Nashville, TN 37232, United States. ²Eugene Bell Center for Regenerative Biology and Tissue Engineering, The Marine Biological Laboratory, Woods Hole, MA 02543, United States. ³Institute of Neurobiology, University of Puerto Rico Medical Sciences Campus, San Juan, PR 00901, United States. ⁴Center for Quantitative Sciences, Vanderbilt University Medical Center, Nashville, TN 37232, United States. ⁵Department of Pharmacology, Vanderbilt University School of Medicine, Nashville, TN 37232, United States. Correspondence and requests for materials should be addressed to R.B.E. (email: ron.emeson@vanderbilt.edu)

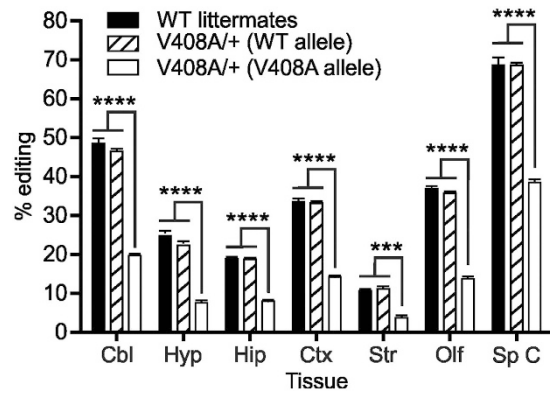


Figure 2. Quantitative analysis of allele-specific Kv1.1 editing in V408A mutant mice. The extent of editing for the wild-type and mutant alleles in heterozygous V408A adult mice (V408A/+), compared to wild-type littermates, was determined for RNA isolated from dissected brain regions and spinal cord by high-throughput sequence analysis (mean \pm SEM, $n = 4$, *** $p \leq 0.001$, **** $p \leq 0.0001$). Cbl, cerebellum; Hyp, hypothalamus; Hip, hippocampus; Ctx, cortex; Str, striatum; Olf, olfactory bulb; Sp C, spinal cord.

sequence was sufficient to decrease the editing rate for Kv1.1 transcripts *in vitro*. Furthermore, the magnitude of this rate decrease corresponded to the proximity of the mutation to the editing site (I400 V), with the most severe deficit observed for the V404I mutation (81% rate reduction at 2 nM RNA), and a 58% and 17% reduction in editing rate for the I407M and V408A mutations, respectively.

A mouse model of EA1 (V408A/+) alters RNA editing *in vivo*. To date, only one mouse model of EA1 has been developed³⁴. Mutant mice homozygous for the V408A allele die between embryonic day 3 (E3) and E9, whereas V408A/+ heterozygotes are characterized by stress-induced ataxia as well as attenuated cerebellar Purkinje signaling, which has been attributed to action potential broadening at basket cell boutons leading to increased GABA release^{34,35}. To determine whether the presence of the V408A mutation inhibited Kv1.1 editing *in vivo*, we isolated RNA from multiple dissected brain regions and spinal cord of wild-type and V408A/+ mutant animals to determine RNA editing profiles by high-throughput sequence analysis of Kv1.1 transcripts. Since this deep-sequencing approach generates sequence reads covering both the V408A mutation and the editing site, it was possible to quantify allele-specific editing profiles in V408A/+ heterozygotes. Results from this analysis indicated that the extent of editing for the wild-type allele in V408A/+ mutant mice was similar to that observed in wild-type animals. Editing for the mutant V408A allele showed a 59% reduction in site-specific editing efficiency in all tissues examined when compared to either wild-type littermates or the V408A/+ wild-type allele (Fig. 2).

Gating properties are altered between non-edited and edited Kv1.1 channels harboring EA1 mutations. All three EA1 mutations can affect the rate of editing *in vitro* and the V408A allele can reduce the extent of editing *in vivo* (Figs 1b and 2). Although editing and EA1 mutations separately have been shown to alter the biophysical properties of Kv1.1 channels, it is unknown whether editing may cause unique effects when paired with these EA1-associated mutations. Similarly, it is unclear whether the phenotypic alterations observed in patients bearing the V404I, I407M, or V408A mutations result from changes in channel function mediated by these missense mutations alone or in concert with their effects upon editing. To address these questions, *Xenopus* oocytes were injected with *in vitro* transcribed RNAs encoding either the non-edited (N) or edited (E) isoforms of the wild-type, V404I, I407M, or V408A Kv1.1 subunits, expressed as homotetramers.

The voltage dependence of activation for each channel subtype was analyzed to determine editing-dependent changes, and representative traces for each channel are shown in Fig. 3a. The relationship between macroscopic conductance and voltage was quantified for each channel type. For most constructs, this was derived from normalized tail current measurements; however, V408A E closed too quickly for accurate measurements of tail currents so conductance was measured using outward currents (see equation (1) in *Materials & Methods*). Conductance (G) versus voltage (V) curves were fit to a Boltzmann function, equation (2),

$$G = \frac{1}{1 + e^{\frac{V_{1/2} - V}{k}}} \quad (1)$$

to estimate the midpoint of channel activation ($V_{1/2}$) and the relative voltage sensitivity (k) (Table 1). Consistent with previous reports for I407M N channels²², we observed a 30 mV positive shift in the $V_{1/2}$, but this change was not influenced by editing (Fig. 3b and Table 1). By contrast, V404I also caused a positive shift, but it was more pronounced for the non-edited channel (a shift of 22.1 mV for the non-edited channel, 14.2 mV for the edited channel; Fig. 3c and Table 1). Thus, editing partially ameliorated the alteration in channel function caused by the V404I mutation. V408A channels did not exhibit altered voltage-dependence for either the non-edited or edited isoforms (Supplementary Fig. S1 and Table 1). Editing had little effect on voltage sensitivity for any of the wild-type or mutant homotetrameric channels (Table 1).

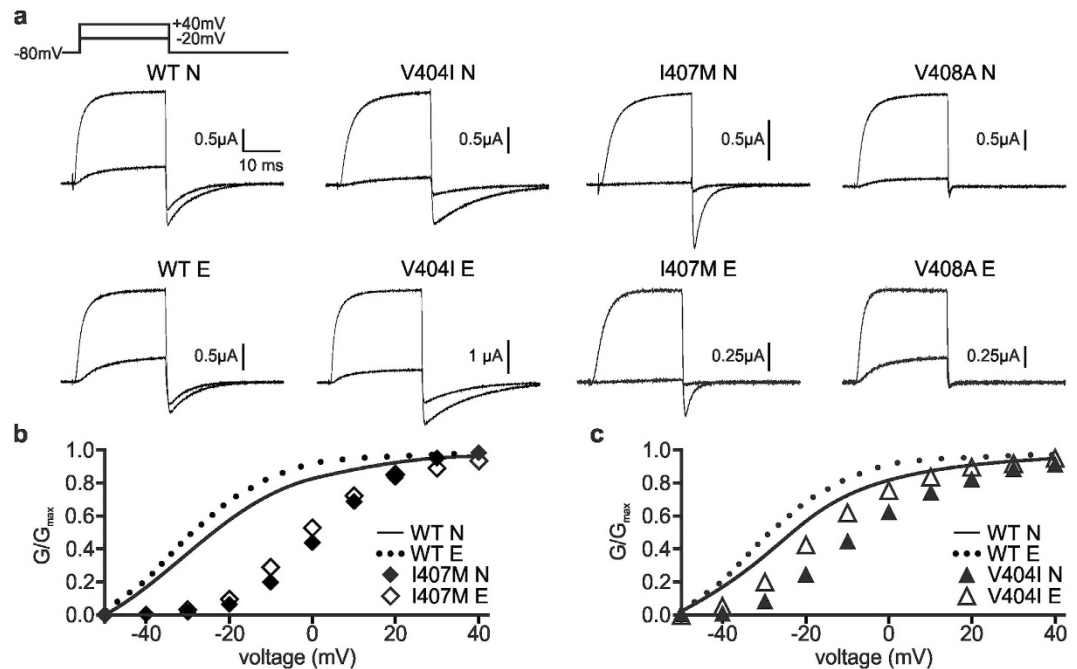


Figure 3. Voltage-dependence of non-edited compared to edited mutant channels. Whole-cell K^+ currents were recorded from oocytes expressing either the non-edited (N) or edited (E) isoforms of homotetrameric wild-type (WT), V404I, I407M, or V408A Kv1.1 channels. Test potentials were elicited in 10 mV voltage steps from -50 to 40 mV, from a holding potential of -80 mV. (a) Representative activating traces at -20 and 40 mV are shown for each construct. (b,c) Conductance (G) versus voltage plots are shown where data have been normalized to the maximal conductance (G_{max}), demonstrating shifts in voltage dependence for (b) I407M and (c) V404I (mean \pm SEM, $n = 4-8$ oocytes). Normalized conductance was measured from tail current amplitude. Small error bars were obscured by the data symbols.

	$V_{1/2}$ (mV)		k (mV)	
WT N	-31.6 ± 1.7		16.0 ± 0.9	
WT E	-34.5 ± 2.3		12.3 ± 1.4	
V404I N	-9.5 ± 1.4	****	14.7 ± 1.1	
V404I E	-20.3 ± 1.5	***	14.2 ± 0.9	
I407M N	-1.9 ± 0.8	****	10.7 ± 0.2	***
I407M E	2.5 ± 1.1	****	9.4 ± 0.2	***
V408A N	-29.4 ± 0.9		9.1 ± 1.0	***
V408A E	-23.6 ± 3.4		8.1 ± 0.4	

Table 1. Voltage-dependence of activation. Voltage-dependence of activation was determined by fitting data to a Boltzmann function, equation (2), to determine the midpoint of channel activation ($V_{1/2}$) and relative voltage sensitivity (k). All data are represented as mean \pm SEM, $n = 4-8$ oocytes for each channel type. Edited (E) and non-edited (N) isoforms of the mutant channels were compared to WT E and WT N channels, respectively: *** $p \leq 0.001$; **** $p < 0.0001$. All types of N channels were compared to their respective E channels: ++ $p \leq 0.005$; +++ $p \leq 0.001$. Due to multiple comparisons, significance was set at $p \leq 0.005$.

To examine how editing affected channel opening kinetics, the time to reach half-maximal activation across a range of voltages was determined. The only editing-dependent change was observed for the I407M mutation. Both I407M channels opened more slowly than their wild-type counterparts, but the slowing was more severe for I407M E channels (Fig. 4a,b and Supplementary Fig. S2), leading to channels with an exacerbated slow opening phenotype. In addition, I407M E and V408A E channels demonstrated non-linearity in their voltage dependence for outward currents, particularly at very positive voltages, reaching peak current amplitudes at 50 and 40 mV respectively, with further voltage steps resulting in decreasing current amplitudes (Supplementary Fig. S3).

Closing (deactivation) kinetics were measured by fitting single exponential curves to tail current traces to obtain estimates of τ , the reciprocal of the closing rate constant. Editing resulted in wild-type channels closing slightly faster (Supplementary Fig. S4). In addition, the I407M and V408A mutations greatly increased closing speeds on their own. The editing of I407M channels had only a small effect on deactivation kinetics, while the edited V408A channels closed so quickly that the closing rate could not be accurately measured

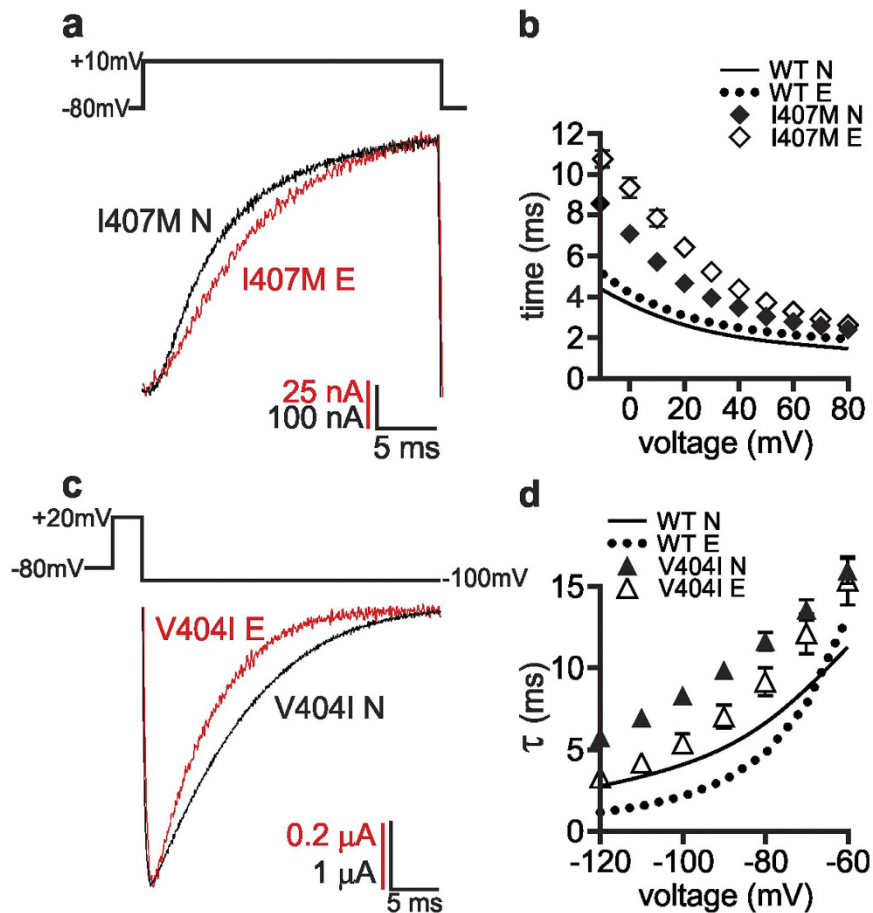


Figure 4. Editing alters gating kinetics of I407M and V404I channels. (a) Representative activation traces, depicting whole-cell currents, were recorded from oocytes expressing either the I407M N or I407M E channel. Test potentials were elicited in 10 mV voltage steps from -10 to 80 mV, from a holding potential of -80 mV. (b) Activation kinetics were measured as the time to reach half-maximal current amplitude (mean \pm SEM, $n = 3-7$ oocytes). I407M N and I407M E channels were significantly slowed in their time to half-activation compared to each other, in the voltage range -10 to 70 mV ($0.05 > p \geq 0.0008$). I407M N was significantly slower than WT N at all voltages ($p \leq 0.0001$) and I407M E was significantly slower than WT E at all voltages ($0.01 > p \geq 0.0001$). (c) Representative tail current traces, depicting whole-cell K^+ currents, were recorded from oocytes expressing either the V404I N or V404I E channel. Following a holding potential of -80 mV and a depolarizing pulse to 20 mV, test potentials were elicited in 10 mV voltage steps from -120 to -60 mV. (d) Closing kinetics were determined by fitting the tail currents with single exponential curves to determine the associated τ value; (mean \pm SEM, $n = 3-6$ oocytes). V404I N channels closed slower than V404I E from -120 to -100 mV ($0.05 > p \geq 0.0066$). V404I N channels closed slower than WT N at all voltages ($p < 0.0001$) and V404I E channels closed significantly slower than WT E channels from -120 to -80 mV ($0.01 \geq p \geq 0.0005$). Small error bars were obscured by the data symbols in some cases.

(Supplementary Fig. S4). Unlike the other mutations, however, V404I led to slower closing speeds and editing partially ameliorated this phenotype (Fig. 4c,d).

Slow inactivation (C-type) was examined by analyzing channel function under conditions of long depolarizations. The I407M E and V408A E channels demonstrated editing-dependent dysfunction, with a prominent fast component of their inactivation appearing alongside the slow component. Thus, while a single exponential function was sufficient to describe the inactivation for the majority of the channels, I407M E and V408A E required a double exponential fit (Supplementary Fig. S5a). Both the fast and slow components of the I407M E and V408A E channels were fast compared to their non-edited counterparts (Supplementary Fig. S5b). By contrast, the extent of inactivation was predominantly mutation-driven, except for the V408A mutation, in which editing decreased the extent of inactivation, bringing it closer to wild-type levels (Supplementary Fig. S5c).

Inactivation kinetics are altered between non-edited and edited EA1 mutant proteins. Previous studies by Bhalla *et al.*¹⁵ found that the most profound change in channel function between non-edited and edited isoforms of the wild-type Kv1.1 channel was a change in the rate of recovery from channel inactivation, presumably by altering interactions with an inactivating Kv β subunit. To determine the effect of EA1 mutations on this

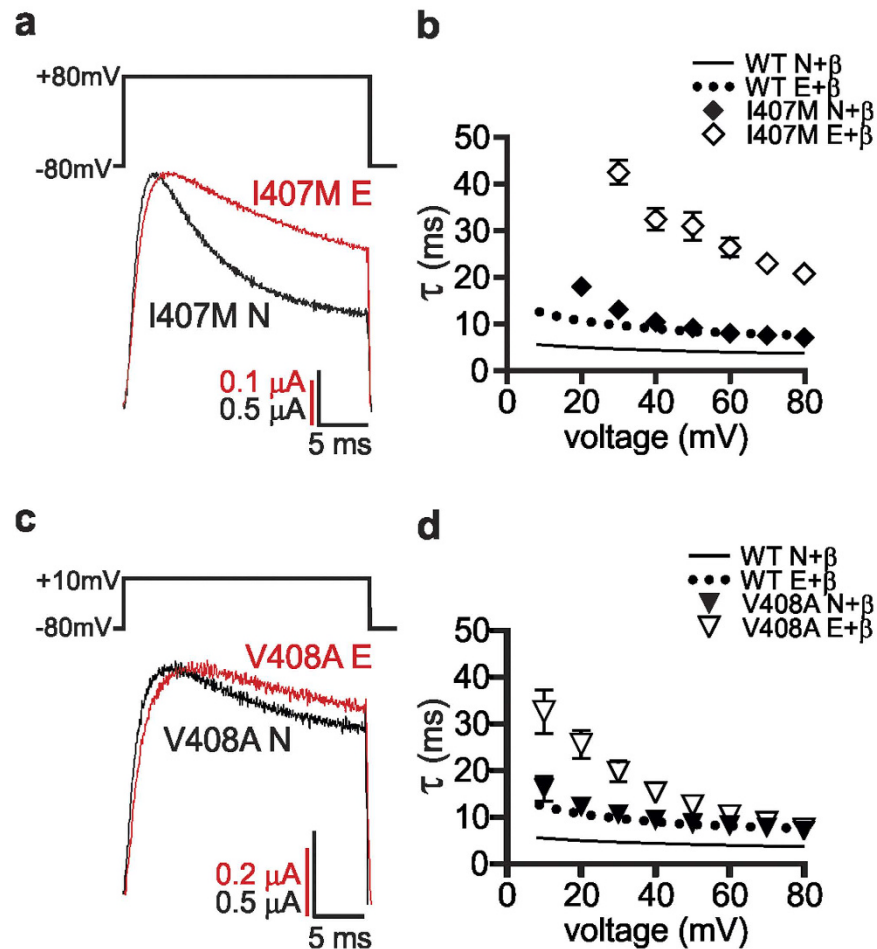


Figure 5. Editing slows Kv β 1.1-induced inactivation kinetics of I407M and V408A channels.

(a,c) Representative β -inactivation traces, depicting whole-cell K^+ currents, were recorded from oocytes co-expressing the Kv β 1.1 subunit and either the (a) I407M or (c) V408A channel, in the non-edited (N) or edited (E) isoform. Test potentials were elicited in 10 mV voltage steps from 10 to 80 mV, from a holding potential of -80 mV. (b,d) Inactivation kinetics were measured by fitting single exponential curves to the test pulse currents, to determine the associated τ value (mean \pm SEM, $n = 3$ –6 oocytes). (b) I407M E channels were significantly slower to inactivate than I407M N channels at every voltage ($p \leq 0.0001$) and both I407M N and I407M E channels were slower than WT N and WT E channels, respectively, at every voltage ($p \leq 0.0001$). (d) V408A E channels were significantly slower than V408A N channels from 10 to 50 mV ($0.05 > p \geq 0.0005$). V408A E channels were slower than WT E channels from 10 to 60 mV ($0.05 > p \geq 0.0001$). V408A N channels were significantly slower than WT N channels at all voltages ($p \leq 0.0001$). Small error bars were obscured by the data symbols in some cases.

biophysical property, non-edited and edited isoforms of the wild-type, V404I, I407M, and V408A channels were co-expressed with Kv β 1.1 to measure N-type, fast inactivation kinetics and recovery from inactivation.

Oocytes expressing each channel subtype, along with Kv β 1.1, were subjected to short depolarizing pulses to different voltages and the resulting fast inactivation traces were fit to a single exponential. These studies identified a previously uncharacterized difference in wild-type channels where editing modestly slowed the rate of channel inactivation (Supplementary Fig. S6). V404I N and E channels inactivated within the wild-type range, without exhibiting any editing-dependent changes (Supplementary Fig. S6). Inactivation for non-edited isoforms of the I407M and V408A mutants resembled edited, wild-type channels, however, editing of I407M and V408A resulted in drastically slower rates of inactivation for both channels (Fig. 5). This effect was most extreme and apparent at all voltages for I407M E, whereas slowing was only observed for V408A E with shallow depolarizations. Interestingly, the V404I N channels also exhibited a low extent of inactivation where inactivation could not be measured in over half the oocytes tested (*data not shown*). This variability in the extent of inactivation for the mutant channels is consistent with previous studies demonstrating that the extent of inactivation could be manipulated by varying the aliphatic amino acid residues at the position of the editing site¹⁷.

Long depolarizing pulses were measured to determine the fast and slow components of Kv1.1 channels when co-expressed with Kv β 1.1 (Supplementary Fig. S7a). Double exponential curves were fit to the inactivating traces, to determine the fast and slow τ values and the relative amplitude of the fast component of the inactivation

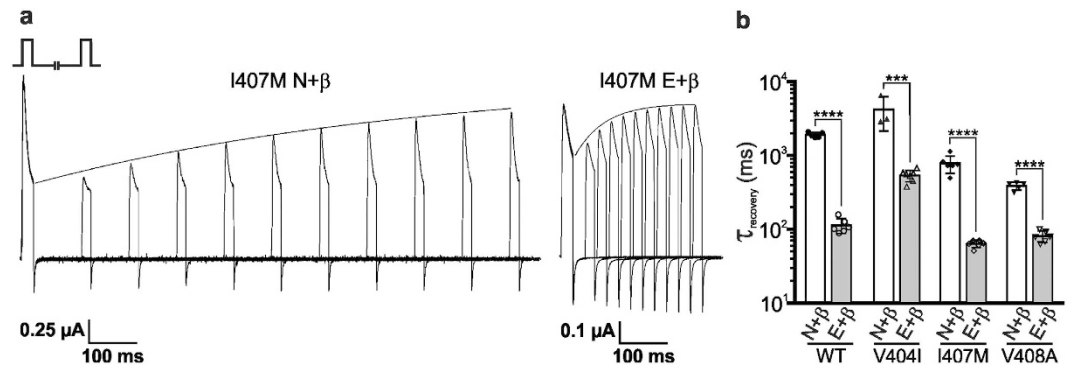


Figure 6. Editing alters the recovery from Kv β 1.1-induced inactivation in V404I, I407M, and V408A channels. Whole-cell K⁺ currents were recorded from oocytes co-expressing the Kv β 1.1 subunit and either a non-edited (N) or edited (E) isoform of the wild-type (WT) or mutant Kv1.1 channel. **(a)** Representative I407M N and I407M E recovery traces are overlaid to depict the increased rate of recovery from β -inactivation, typical of an E isoform. A two-pulse protocol was used, eliciting a depolarizing pulse to 80 mV followed by a variable interpulse duration at -80 mV before a final depolarizing pulse at 80 mV. Recovery from β -inactivation was plotted as the time for the second pulse to regain the current amplitude of the first pulse. **(b)** τ values were determined by fitting single exponential curves to the recovery plots (mean \pm SEM, $n = 3-7$ oocytes, *** $p \leq 0.001$, **** $p \leq 0.0001$).

(compared to the slow component). The fast and slow τ values largely corresponded to the results described for the β -inactivation of the short pulses and the slow inactivation of the long pulses without Kv β 1.1 (*data not shown*). In wild-type channels, editing led to an increase in the relative amplitude of the fast component of inactivation. An editing-dependent change also was observed for the V404I channels, where editing brought the relative amplitude of the fast component closer to that of the wild-type channel (Supplementary Fig. S7b).

Finally, the rate of recovery from fast inactivation was measured using a two-pulse protocol, where the fractional recovery at specific time intervals was assessed after the onset of inactivation. A representative experiment for oocytes expressing either I407M N or E channels is presented in Fig. 6a. As previously reported in Bhalla *et al.*¹⁵, editing increased the rate of recovery when comparing non-edited and edited isoforms of the wild-type channel (Fig. 6b). All edited isoforms of the mutant channels exhibited a significantly faster rate of recovery than their respective non-edited counterparts (Fig. 6b and Supplementary Table S1). Recovery from inactivation for the V404I E channel was significantly slower than that of the WT E channel, whereas for the I407M N, I407M E, and V408A N channels it was faster compared to its corresponding wild-type channel. Although the extent of the effect differed for each mutation, editing resulted in a unique and substantial contribution to the rate of recovery from fast-inactivation for each channel type.

Discussion

The conversion of A-to-I by RNA editing has been shown to represent an important post-transcriptional modification by which to modulate the function of numerous proteins critical for nervous system function³⁶. Previous studies have shown that site-selective editing of transcripts encoding the Kv1.1 channel can affect the rate of recovery from channel inactivation, the binding of drugs and highly unsaturated fatty acids, the regulation of homotetrameric Kv1.1 channel trafficking, and seizure-susceptibility in chronic epileptic rats^{15,17,37-39}. While numerous EA1-associated mutations have been identified throughout the *KCNA1* coding region, several of these mutations (V404I, I407M, and V408A) are within close proximity to the Kv1.1 editing site (I400V) and also are predicted to disrupt the critical RNA duplex structure required for this post-transcriptional modification.

To our knowledge, the present studies represent the first demonstration that disease-associated mutations can disrupt critical *cis*-regulatory elements to change their gene's RNA editing profile, by altering the RNA structure required for site-selective A-to-I conversion. Results using both *in vitro* and *in vivo* model systems have shown significant reductions in the extent and rate of editing for Kv1.1 transcripts harboring specific EA1 mutations (Figs 1b and 2). Importantly, because the wild-type allele RNA was unchanged in the V408A/+ mouse model, it is likely that the observed changes in the editing of the V408A allele-derived RNA were solely due to the V408A mutation and not due to any developmental, compensatory changes. Our studies suggest that both synonymous and non-synonymous duplex-disrupting mutations and single nucleotide polymorphisms within Kv1.1 and other edited RNA targets may also affect the expression of their specific edited isoforms, thus altering the activity of the encoded protein products.

These studies also have revealed that the effects of EA1 mutations on Kv1.1 function are far more complex than originally anticipated, as each mutation produces channels with unique biophysical properties that depend on the I400V amino acid identity, mediated by RNA editing. The V404I mutation altered several electrophysiological parameters on its own, but the edited isoform demonstrated less drastic changes than the non-edited isoform, as observed for channel voltage sensitivity, closing kinetics, and the amplitude of β -inactivation (Figs 3c and 4c,d, Supplementary Fig. S7). Although it is tempting to speculate that editing could dampen the defects in channel function resulting from this point mutation, it also should be noted that this mutation largely

prevents the RNA from being edited in the first place (Fig. 1b). Thus, it is anticipated that edited V404I isoforms contribute little to the electrophysiological properties of Kv1.1 channels in those tissue where they are expressed. Unlike the V404I channel, however, editing combined with the I407M or V408A mutations led to more severe channel dysfunctions than the non-edited isoforms. Edited isoforms of both I407M and V408A exhibited unusually slow β -dependent inactivation kinetics (Fig. 5) and severe defects in activation at higher voltages (Supplementary Fig. S3) that could possibly be caused by a significantly faster entry into, or slower recovery from, C-type inactivation (Supplementary Fig. S5)⁴⁰. In addition, while the I407M mutation slowed the kinetics of channel opening, the effect was greater for the edited isoform (Fig. 4a,b). These studies also extended the characterization of the I407M mutation, as previous studies of the non-edited I407M channel reported only alterations in expression and voltage-sensitivity⁴¹, while the present study also shows changes in kinetics (Fig. 4a,b and 5). Further characterizations of edited EA1 mutant channels could help us better understand their physiological defects *in vivo*. These include stimulating the channels with action potential-like commands (trains of depolarizing pulses) to assess cumulative inactivation, as well as probing the voltage-dependence of their inactivation. Since these mutations also led to decreases in the editing of Kv1.1 transcripts, additional experiments will be required to test the relative contribution of editing-dependent and independent effects, especially when the Kv1.1 proteins are co-assembled into heterotetramers with other Kv1.x family members^{20,41,42}.

Although our studies suggest that edited isoforms of mutant channels represent a smaller portion of the total Kv1.1 population, they may still exert functional effects, particularly in tissues with higher editing levels (such as cerebellum and spinal cord) (Fig. 2). This is supported by previous studies, which have shown that incorporating even one edited subunit into a Kv1.x heterotetramer was sufficient to alter its sensitivity to open-channel blocking molecules³⁷. Alternatively, despite the many functional differences observed between edited isoforms of the mutant channels, all recovered from fast inactivation significantly faster than their non-edited counterparts (Fig. 6). As these EA1 mutations reduced their own isoform editing, it is predicted that the overall recovery from fast inactivation *in vivo* will be comparatively slow, possibly resulting in unanticipated effects that could prevent normal neuronal signaling.

While no clear correlation has been established between the diverse clinical phenotypes of EA1 patients and specific mutations within Kv1.1^{18–27}, part of the observed variability in symptoms might be explained by differences in RNA editing. These phenotypic differences could arise from EA1 mutations that disrupt the editing duplex, or from overall changes in Kv1.1 editing regulation. Although the mechanisms regulating Kv1.1 RNA editing are largely unknown, recent studies have demonstrated that inducing rats with chronic epilepsy led to a 4-fold increase in Kv1.1 editing in the entorhinal cortex³⁸. Interestingly, once Kv1.1 editing was increased, recordings in isolated rat brain slices demonstrated that these animals had a decreased sensitivity to 4-aminopyridine-induced seizure-like events, suggesting that increasing editing might dampen seizure susceptibility. Similarly, analyses of patients undergoing surgery for mesial temporal lobe epilepsy revealed that having increased levels of Kv1.1 RNA editing was negatively correlated with the period of years that the patients had experienced epileptic activity⁴³, suggesting that decreased Kv1.1 editing may represent a risk factor for long-term seizures. Graves *et al.*²⁷ clinically surveyed two families containing the same EA1 mutation (F414S), and found that one family exhibited seizures while the other did not, raising the possibility that additional factors, such as differences in editing regulation, could represent an explanation for these phenotypic differences. As previous studies have shown that open-channel blocking drugs interact less with edited Kv1.1 homo- and heterotetramers³⁷, a precise therapeutic strategy for the treatment of Kv1.1-dependent seizures may require not only a knowledge of the specific mutation(s) involved, but also the editing profiles of Kv1.1 transcripts.

Materials and Methods

Kv1.1 and Kv β 1.1 constructs. A 463 bp-region encompassing the duplex required for Kv1.1 editing was amplified using the polymerase chain reaction (PCR) from human genomic DNA using sense (5'-GCGAAGCTTCTCTTCATCGGGGTCATCCT-3') and antisense (5'-GCGGCGGCCGAGTTTTGGTTAGCAGTGG-3') oligonucleotide primers in exon 2. To aid in subcloning, the primers incorporated Hind III and Not I restriction sites on their 5'-ends for the sense and antisense primers, respectively. The PCR amplicon was subcloned into the mammalian expression vector, pRc-CMV (Thermo Fisher) to generate a wild-type Kv1.1 minigene. To generate the V404I, I407M, and V408A minigenes, the wild-type Kv1.1 construct was mutagenized using the QuikChange II Site-Directed Mutagenesis kit (Agilent Technologies), where the PCR reactions were supplemented with 5% DMSO. Full-length mouse Kv1.1 (Addgene) and mouse Kv β 1.1 (Thermo Scientific) cDNAs were subcloned into the *Xenopus* expression vector, pGEM HE⁴⁴. The following full-length constructs were created by PCR mutagenesis from the full-length mouse non-edited Kv1.1 cDNA and validated by sequence analysis: wild-type edited Kv1.1 and V404I, I407M, and V408A mutant Kv1.1 (non-edited and edited) cDNAs.

***In vitro* analysis of RNA editing.** RNAs were transcribed *in vitro* from the wild-type Kv1.1 minigene, as well as corresponding minigenes harboring the V404I, I407M, and V408A mutations using the MAXiScript kit (Ambion) with T7 RNA polymerase according to manufacturer's instructions. Nuclear extracts were prepared from transiently transfected HEK293 cells expressing rat ADAR2, as described previously, and stored at -80°C until required^{32,45}. Immediately prior to *in vitro* editing analysis, nuclear extracts were diluted 1:10 in dialysis buffer [20 mM HEPES, 1 mM EDTA, 1 mM EGTA, 10% glycerol, 300 mM NaCl, 1 mM PMSF, 1 mM DTT, 1X complete, EDTA-free protease inhibitor cocktail (Roche)], before a 2-hour incubation at 30°C with RNase inhibitors and RNA substrates varying in concentration from 0.125 to 2 nM. Nuclear extracts represented one-third of the total 50 μL reaction volume which was diluted with the RNA substrate and water to reduce the glycerol concentration into a range necessary for ADAR2 activity. The incubation time was determined empirically by time-course analyses to ensure that editing of the wild-type Kv1.1 minigene was within the linear range of the reaction (*data not shown*). Reactions were terminated by the addition of TRIzol (Ambion) and RNA was

extracted according to the manufacturer's protocol. RNA was reverse-transcribed with random primers using the High Capacity cDNA Reverse Transcription kit (Applied Biosystems) and the extent of RNA editing was quantified by high-throughput multiplexed sequence analysis as described previously³³. The editing rate was calculated as the fmol RNA converted to the edited isoform divided by the duration of the reaction.

In vivo analysis of RNA editing. All animal care and experimental procedures involving mice were approved by the Vanderbilt University Medical Center Institutional Animal Care and Use Committee and were performed in accordance with relevant guidelines and regulations. Mice harboring the heterozygous V408A mutation (V408A/+) were generously provided by Dr. James Maylie (Oregon Health & Science University)³⁴. At approximately 6 weeks of age, male V408A/+ and wild-type littermates were euthanized by cervical dislocation under anesthesia followed by decapitation. Six brain regions (cerebellum, hippocampus, hypothalamus, cortex, striatum, olfactory bulb) and spinal cord were dissected from each mouse. Tissues were flash-frozen in liquid nitrogen and RNA was isolated by sonication in TRIzol (Ambion) according to the manufacturer's instructions. RNA was reverse-transcribed and Kv1.1 editing was quantified by high-throughput sequence analysis as described for *in vitro* RNA editing analyses.

Electrophysiological recording in *Xenopus* oocytes. All animal care and experimental procedures involving *Xenopus laevis* were approved by the University of Puerto Rico Institutional Animal Care and Use Committee and were performed in accordance with relevant guidelines and regulations. Kv β 1.1 and full-length, wild-type, V404I, I407M, and V408A Kv1.1 RNAs were transcribed *in vitro*, capped, and polyadenylated using the T7 mScript Standard mRNA Production System (CELLSCRIPT). Ovary sections containing several hundred oocytes were removed from adult specimens of *Xenopus laevis* obtained from Xenopus Express (Brooksville, FL). Oocytes were dispersed with type II collagenase and manually defolliculated. Stage V and VI oocytes were then selected by manual inspection for subsequent RNA injection. On day 1, oocytes were injected with 38.6 nL of one of the eight full-length Kv1.1 RNAs encoding edited and non-edited isoforms of wild-type, V404I, I407M, and V408A channels, with or without the Kv β 1.1 RNA. Injection concentrations were optimized individually for each construct, with greater concentrations required for the I407M and V408A RNAs due to protein expression differences previously described in the literature^{21,22}. Each α -subunit was injected at a concentration from 2 ng/ μ L to 1 μ g/ μ L and co-injected with Kv β 1.1 when applicable; concentrations for the Kv β 1.1 constructs were 10-fold more than each α -subunit, up to a maximum injection concentration of 500 ng/ μ L. Electrophysiological analysis of oocytes were performed between day 3–5 post-injection using the cut-open oocyte voltage-clamp technique⁴⁶. The external solution consisted of: 20 mM K-glutamate, 100 mM L-glutamate, 2.5 mM MgCl₂, 2.5 mM CaCl₂, 10 mM HEPES, pH 7.4. The internal solution consisted of: 120 mM K-glutamate, 2.5 mM EGTA, 10 mM HEPES, pH 7.4. The pH of the solutions was adjusted using N-methyl-D-glucamine, as an alternative to NaOH, to limit the introduction of sodium ions into the solutions. To gain electrical access to the oocyte interior, the internal solution was supplemented with 0.3% saponin and used for a brief permeabilization prior to recording. The oocyte membrane potential was controlled using a CA-1B High Performance Oocyte Clamp (Dagan Corporation). Analog current signals were digitized at 100 kHz using an SBC6711 A/D D/A board (Innovative Integration, Simi Valley CA) and filtered at 5 kHz. To avoid errors introduced by series resistance, only traces exhibiting less than 10 μ A were used for analysis. GPATCH M software, kindly provided by Dr. F. Bezanilla (University of Chicago), was used for data collection and clamp control. Leak currents were subtracted using a linear P/4 procedure. Data were analyzed using ANALYSIS software, also provided by Dr. F. Bezanilla, for fitting data with exponential functions and measuring current amplitudes. In addition, single exponential curves were fitted to recovery from the inactivation data using Graphpad Prism (Graphpad Software) to determine the rate constant, τ . As the channels encoded by edited V408A transcripts closed too rapidly for measurements of tail current amplitude, conductance (G) was calculated using Ohm's law, equation (1),

$$G = \frac{I}{V - V_r} \quad (2)$$

where I represents the maximal current at the test potential (V) and V_r signifies the reversal potential, determined empirically. For Figs 3–6 and Supplementary Figures S5 and S7, points arising from brief capacity transients were removed for clarity.

Statistical analysis. Statistical comparisons for *in vitro* (Fig. 1b) and *in vivo* (Fig. 2) editing analyses were determined by 2-way ANOVA with Tukey's multiple comparisons test. Boltzmann functions were fitted using non-linear regression to model conductance-voltage curves (Fig. 3 and Supplementary Fig. S1) and to determine $V_{1/2}$ and k values associated with each replicate (Table 1). Two-sample Student's t-tests were used to compare voltage-dependent parameters (Table 1), long pulse characterization with and without Kv β 1.1 (Supplementary Figs S5 and S7), and recovery from inactivation τ values (Fig. 6b and Supplementary Table S1). The above analyses were conducted using Graphpad Prism (Graphpad Software). To maintain the type I error rate for each experiment at 5%, a Bonferroni correction was applied to each test based on the number of comparisons within each experiment and statistical significance for any pair of treatment comparisons was redefined according to these adjusted p-values. For Table 1 and Supplementary Table S1, 10 comparisons were made and the significance was adjusted to $p \leq 0.005$. For Supplementary Figure S5b, 42 comparisons were made and the significance was adjusted to $p \leq 0.0012$. For Supplementary Figures S5c and S7b, 30 comparisons were made and the significance was adjusted to $p \leq 0.0017$. Analysis of activation and deactivation (Fig. 4 and Supplementary Figs S2 and S4), and inactivation kinetics (Fig. 5 and Supplementary Fig. S6) were performed with linear mixed models using the natural log of the acquired data to better meet model assumptions. Individual

group comparisons for p-values were based on the Wald tests of model-based predicted (least square) means and appropriate standard errors. Because these data indicate that the measurements of activation, deactivation, and β -inactivation were dependent on voltage, comparisons were made only between values obtained at the same voltage. Data are presented with their original scale to allow for easier interpretation and comparison with the existing EA1 literature. All statistical tests were two-sided and statistical significance was defined as $p \leq 0.05$, unless a specified Bonferroni correction was applied.

References

- Robbins, C. A. & Tempel, B. L. Kv1.1 and Kv1.2: Similar channels, different seizure models. *Epilepsia* **53**, 134–141, doi: 10.1111/j.1528-1167.2012.03484.x (2012).
- Ishikawa, T. *et al.* Distinct Roles of Kv1 and Kv3 Potassium Channels at the Calyx of Held Presynaptic Terminal. *J. Neurosci.* **23**, 10445–10453 (2003).
- Smart, S. L. *et al.* Deletion of the KV1.1 Potassium Channel Causes Epilepsy in Mice. *Neuron* **20**, 809–819, doi: 10.1016/s0896-6273(00)81018-1 (1998).
- Clark, J. D. & Tempel, B. L. Hyperalgesia in mice lacking the Kv1.1 potassium channel gene. *Neurosci. Lett.* **251**, 121–124 (1998).
- Glasscock, E., Yoo, J. W., Chen, T. T., Klassen, T. L. & Noebels, J. L. Kv1.1 potassium channel deficiency reveals brain-driven cardiac dysfunction as a candidate mechanism for sudden unexplained death in epilepsy. *J. Neurosci.* **30**, 5167–5175, doi: 10.1523/JNEUROSCI.5591-09.2010 (2010).
- Coleman, S. K., Newcombe, J., Pryke, J. & Dolly, J. O. Subunit Composition of Kv1 Channels in Human CNS. *J. Neurochem.* **73**, 849–858, doi: 10.1046/j.1471-4159.1999.0730849.x (1999).
- Koch, R. O. *et al.* Complex Subunit Assembly of Neuronal Voltage-gated K⁺ Channels Basis for High-Affinity Toxin Interactions and Pharmacology. *J. Biol. Chem.* **272**, 27577–27581, doi: 10.1074/jbc.272.44.27577 (1997).
- Rasband, M. N. *et al.* Distinct potassium channels on pain-sensing neurons. *Proc. Natl. Acad. Sci. USA* **98**, 13373–13378, doi: 10.1073/pnas.231376298 (2001).
- Sokolov, M. V., Shamotienko, O., Dhochartaigh, S. N., Sack, J. T. & Dolly, J. O. Concatemers of brain Kv1 channel alpha subunits that give similar K⁺ currents yield pharmacologically distinguishable heteromers. *Neuropharmacol.* **53**, 272–282, doi: 10.1016/j.neuropharm.2007.05.008 (2007).
- Parcej, D. N., Scott, V. E. & Dolly, J. O. Oligomeric properties of alpha-dendrotoxin-sensitive potassium ion channels purified from bovine brain. *Biochemistry* **31**, 11084–11088 (1992).
- Rhodes, K. J. *et al.* Association and Colocalization of the Kv β 1 and Kv β 2 β -Subunits with Kv1 α -Subunits in Mammalian Brain K⁺ Channel Complexes. *J. Neurosci.* **17**, 8246–8258 (1997).
- Rettig, J. *et al.* Inactivation properties of voltage-gated K⁺ channels altered by presence of beta-subunit. *Nature* **369**, 289–294, doi: 10.1038/369289a0 (1994).
- Zhou, M., Morais-Cabral, J. H., Mann, S. & MacKinnon, R. Potassium channel receptor site for the inactivation gate and quaternary amine inhibitors. *Nature* **411**, 657–661, doi: 10.1038/35079500 (2001).
- Hoopengardner, B., Bhalla, T., Staber, C. & Reenan, R. Nervous System Targets of RNA Editing Identified by Comparative Genomics. *Science* **301**, 832–836, doi: 10.1126/science.1086763 (2003).
- Bhalla, T., Rosenthal, J. J. C., Holmgren, M. & Reenan, R. Control of human potassium channel inactivation by editing of a small mRNA hairpin. *Nat. Struct. Mol. Biol.* **11**, 950–956, doi: 10.1038/nsmb825 (2004).
- Horsch, M. *et al.* Requirement of the RNA-editing enzyme ADAR2 for normal physiology in mice. *J Biol Chem* **286**, 18614–18622, doi: 10.1074/jbc.M110.200881 (2011).
- Gonzalez, C., Lopez-Rodriguez, A., Srikumar, D., Rosenthal, J. J. C. & Holmgren, M. Editing of human KV1.1 channel mRNAs disrupts binding of the N-terminus tip at the intracellular cavity. *Nat. Commun.* **2**, doi: 10.1038/ncomms1446 (2011).
- Graves, T. D. *et al.* Episodic ataxia type 1: clinical characterization, quality of life and genotype–phenotype correlation. *Brain* **137**, 1009–1018, doi: 10.1093/brain/awu012 (2014).
- D'Adamo, M. C. *et al.* New insights into the pathogenesis and therapeutics of episodic ataxia type 1. *Front. Cell. Neurosci.* **9**, 317, doi: 10.3389/fncel.2015.00317 (2015).
- Imbrici, P., D'Adamo, M. C., Kullmann, D. M. & Pessia, M. Episodic ataxia type 1 mutations in the KCNA1 gene impair the fast inactivation properties of the human potassium channels Kv1.4-1.1/Kv β 1.1 and Kv1.4-1.1/Kv β 1.2. *Eur. J. Neurosci.* **24**, 3073–3083, doi: 10.1111/j.1460-9568.2006.05186.x (2006).
- Zerr, P., Adelman, J. P. & Maylie, J. Episodic Ataxia Mutations in Kv1.1 Alter Potassium Channel Function by Dominant Negative Effects or Haploinsufficiency. *J. Neurosci.* **18**, 2842–2848 (1998).
- Tomlinson, S. E. *et al.* Clinical, genetic, neurophysiological and functional study of new mutations in episodic ataxia type 1. *J. Neurol. Neurosurg. Psychiatry* **84**, 1107–1112, doi: 10.1136/jnnp-2012-304131 (2013).
- Eunson, L. H. *et al.* Clinical, genetic, and expression studies of mutations in the potassium channel gene KCNA1 reveal new phenotypic variability. *Ann. Neurol.* **48**, 647–656 (2000).
- Mestre, T. A. *et al.* A novel KCNA1 mutation in a family with episodic ataxia and malignant hyperthermia. *Neurogenetics*, doi: 10.1007/s10048-016-0486-0 (2016).
- Chen, S. H., Fu, S. J., Huang, J. J. & Tang, C. Y. The episodic ataxia type 1 mutation I262T alters voltage-dependent gating and disrupts protein biosynthesis of human Kv1.1 potassium channels. *Sci. Rep.* **6**, 19378, doi: 10.1038/srep19378 (2016).
- Petitjean, D., Kalstrup, T., Zhao, J. & Blunck, R. A Disease Mutation Causing Episodic Ataxia Type I in the S1 Links Directly to the Voltage Sensor and the Selectivity Filter in Kv Channels. *J. Neurosci.* **35**, 12198–12206, doi: 10.1523/JNEUROSCI.1419-15.2015 (2015).
- Graves, T. D. *et al.* Nongenetic factors influence severity of episodic ataxia type 1 in monozygotic twins (Video). *Neurology* **75**, 367–372, doi: 10.1212/WNL.0b013e3181ea9ee3 (2010).
- Maylie, B., Bissonnette, E., Virk, M., Adelman, J. P. & Maylie, J. G. Episodic Ataxia Type 1 Mutations in the Human Kv1.1 Potassium Channel Alter hKv β 1-Induced N-Type Inactivation. *J. Neurosci.* **22**, 4786–4793 (2002).
- Adelman, J. P., Bond, C. T., Pessia, M. & Maylie, J. Episodic ataxia results from voltage-dependent potassium channels with altered functions. *Neuron* **15**, 1449–1454, doi: 10.1016/0896-6273(95)90022-5 (1995).
- Zuker, M. Mfold web server for nucleic acid folding and hybridization prediction. *Nucleic Acids Res.* **31**, 3406–3415, doi: 10.1093/nar/gkg595 (2003).
- SantaLucia, J. Jr. A unified view of polymer, dumbbell, and oligonucleotide DNA nearest-neighbor thermodynamics. *Proc. Natl. Acad. Sci. USA* **95**, 1460–1465 (1998).
- Steffl, R. *et al.* The Solution Structure of the ADAR2 dsRBM-RNA Complex Reveals a Sequence-Specific Readout of the Minor Groove. *Cell* **143**, 225–237, doi: 10.1016/j.cell.2010.09.026 (2010).
- Hood, J. L. *et al.* Reovirus-mediated induction of ADAR1 (p150) minimally alters RNA editing patterns in discrete brain regions. *Mol. Cell. Neurosci.*, doi: 10.1016/j.mcn.2014.06.001 (2014).
- Herson, P. S. *et al.* A mouse model of episodic ataxia type-1. *Nat. Neurosci.* **6**, 378–383, doi: 10.1038/nn1025 (2003).

35. Begum, R., Bakiri, Y., Volynski, K. E. & Kullmann, D. M. Action potential broadening in a presynaptic channelopathy. *Nat. Commun.* **7**, 12102, doi: 10.1038/ncomms12102 (2016).
36. Hood, J. L. & Emeson, R. B. In *Adenosine Deaminases Acting on R. N. A. (ADARs) and A-to-I Editing Current Topics in Microbiology and Immunology* (ed. Charles, E. Samuel) 61–90 (Springer Berlin Heidelberg, 2012).
37. Decher, N. *et al.* RNA editing modulates the binding of drugs and highly unsaturated fatty acids to the open pore of Kv potassium channels. *EMBO J.* **29**, 2101–2113, doi: 10.1038/emboj.2010.88 (2010).
38. Streit, A. K. *et al.* RNA editing of Kv1.1 channels may account for reduced ictogenic potential of 4-aminopyridine in chronic epileptic rats. *Epilepsia* **52**, 645–648, doi: 10.1111/j.1528-1167.2011.02986.x (2011).
39. Streit, A. K., Matschke, L. A., Dolga, A. M., Rinné, S. & Decher, N. RNA Editing in the Central Cavity as a Mechanism to Regulate Surface Expression of the Voltage-gated Potassium Channel Kv1.1. *J. Biol. Chem.* **289**, 26762–26771, doi: 10.1074/jbc.M113.545731 (2014).
40. Sanguinetti, M. C., Jiang, C., Curran, M. E. & Keating, M. T. A mechanistic link between an inherited and an acquired cardiac arrhythmia: HERG encodes the IKr potassium channel. *Cell* **81**, 299–307 (1995).
41. Manganas, L. N. & Trimmer, J. S. Subunit Composition Determines Kv1 Potassium Channel Surface Expression. *J. Biol. Chem.* **275**, 29685–29693, doi: 10.1074/jbc.M005010200 (2000).
42. D'Adamo, M. C., Imbrici, P., Sponcichetti, F. & Pessia, M. Mutations in the KCNA1 gene associated with episodic ataxia type-1 syndrome impair heteromeric voltage-gated K(+) channel function. *FASEB J.* **13**, 1335–1345 (1999).
43. Krestel, H. *et al.* Differences between RNA and DNA due to RNA editing in temporal lobe epilepsy. *Neurobiol. Dis.* **56**, 66–73, doi: 10.1016/j.nbd.2013.04.006 (2013).
44. Liman, E. R., Tytgat, J. & Hess, P. Subunit stoichiometry of a mammalian K⁺ channel determined by construction of multimeric cDNAs. *Neuron* **9**, 861–871 (1992).
45. Schreiber, E., Matthias, P., Müller, M. M. & Schaffner, W. Rapid detection of octamer binding proteins with 'mini extracts', prepared from a small number of cells. *Nucleic Acids Res.* **17**, 6419–6419, doi: 10.1093/nar/17.15.6419 (1989).
46. Stefani, E. & Bezanilla, F. In *Methods Enzymol. Vol. 293 Ion Channels Part B* (ed. P. Michael Conn) 300–318 (Academic Press, 1998).

Acknowledgements

We would like to thank Dr. James Maylie for generously providing the V408A/+ mice, Kathleen M. Patterson for mouse husbandry, Li Peng for cell culture maintenance and transfection, Sonia Soto for *Xenopus* oocytes isolation and Chris Hofmann for critical reading of the manuscript. We also thank the Vanderbilt VANTAGE facility for performing high-throughput sequencing and Xiaojing Wang for analysis of Illumina data. This work was supported by the Vanderbilt Molecular Endocrinology Training Program (T32DK007563; E.A.F.K.), a Ruth L. Kirschstein National Research Service Award (F31NS087911; E.A.F.K.), a Vanderbilt Dissertation Enhancement Grant (E.A.F.K.), and the Vanderbilt Joel G. Hardman Chair in Pharmacology (R.B.E.). Additional support for J.J.C.R. included NINDS (R0111223855, R01NS64259) and the Cystic Fibrosis Foundation Therapeutics (Rosent14XXO). Infrastructural support for J.J.C.R. was provided by NIGMS (P20GM103642), NIMH (G12-MD007600), and NSF (DBI 0115825, DBI 1337284).

Author Contributions

E.A.F.K., J.J.C.R., and R.B.E. designed all experiments. E.A.F.K. generated all constructs, performed all molecular biology experiments, and performed all electrophysiology experiments with J.J.C.R., E.A.F.K. and G.D.A. were responsible for statistical analysis of data. E.A.F.K. wrote the manuscript and all authors contributed to scientific discussion and editing.

Additional Information

Supplementary information accompanies this paper at <http://www.nature.com/srep>

Competing financial interests: The authors declare no competing financial interests.

How to cite this article: Ferrick-Kiddie, E. A. *et al.* Mutations underlying Episodic Ataxia type-1 antagonize Kv1.1 RNA editing. *Sci. Rep.* **7**, 41095; doi: 10.1038/srep41095 (2017).

Publisher's note: Springer Nature remains neutral with regard to jurisdictional claims in published maps and institutional affiliations.



This work is licensed under a Creative Commons Attribution 4.0 International License. The images or other third party material in this article are included in the article's Creative Commons license, unless indicated otherwise in the credit line; if the material is not included under the Creative Commons license, users will need to obtain permission from the license holder to reproduce the material. To view a copy of this license, visit <http://creativecommons.org/licenses/by/4.0/>

© The Author(s) 2017